



Fermi National Accelerator Laboratory

FERMILAB-Conf-96/284-E

DØ

Hadronic Calibration of DØ Calorimetry

Robert Kehoe
Representing the DØ Collaboration
*University of Notre Dame
Notre Dame, Indiana 46556*

*Fermi National Accelerator Laboratory
P.O. Box 500, Batavia, Illinois 60510*

September 1996

Submitted to the *6th International Conference on Calorimetry in High Energy Physics*, Laboratori Nazionali di Frascati (INFN), Frascati, Italy, June 8-14, 1996.

Disclaimer

This report was prepared as an account of work sponsored by an agency of the United States Government. Neither the United States Government nor any agency thereof, nor any of their employees, makes any warranty, express or implied, or assumes any legal liability or responsibility for the accuracy, completeness or usefulness of any information, apparatus, product or process disclosed, or represents that its use would not infringe privately owned rights. Reference herein to any specific commercial product, process or service by trade name, trademark, manufacturer or otherwise, does not necessarily constitute or imply its endorsement, recommendation or favoring by the United States Government or any agency thereof. The views and opinions of authors expressed herein do not necessarily state or reflect those of the United States Government or any agency thereof.

Distribution

Approved for public release: further dissemination unlimited.

Hadronic Calibration of DØ Calorimetry

Robert Kehoe
(representing the DØ Collaboration)

University of Notre Dame
Notre Dame, Indiana 46556, USA

ABSTRACT

The DØ detector is used to study $\bar{p}p$ collisions at the 1.8 TeV center-of-momentum energies available at the Fermilab Tevatron. The heart of the detector is a hermetic calorimeter employing uranium absorber and liquid argon as the ionization sampling medium. Several analyses require a well-understood jet energy scale. This paper describes how this calibration is obtained.

1 Introduction

Jets are now an important part of many analyses and their proper energy calibration in the detector is crucial. At DØ, the uncertainty in jet energy scale is currently the main contribution to the systematic error in our measurements of the inclusive jet cross section and top quark mass. In this paper, we discuss the DØ jet energy scale determination and outline its verification.

The U/LAr sampling calorimeter is the primary subdetector of DØ ¹⁾ used to identify e, γ , jets and missing transverse energy (\cancel{E}_T). Since there is no magnetic field in the inner tracking volume, the calorimeter is also used for the energy measurement of these objects. The calorimeter readout is segmented transversely into ‘towers’ projective to the center of the detector, each of which cover an area of 0.1×0.1 in $\eta - \phi$. The pseudorapidity, η , is defined as $-\ln(\tan(\theta/2))$ where θ is the angle with respect to the proton beam direction, and ϕ is the azimuthal angle. In depth, each tower is segmented into ‘cells’ in three sections: electromagnetic (EM), fine hadronic (FH), and coarse hadronic (CH). A central cryostat (CC) covers

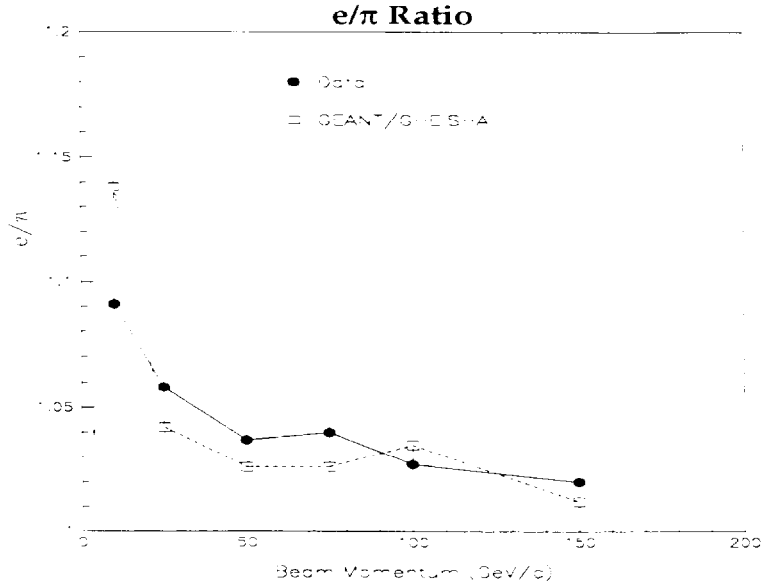


Figure 1: Energy dependence of e/π in EC for GEANT and test beam.

$|\eta| < 1.0$ and two end cryostats (EC) cover $1.0 < |\eta| < 4.0$. At DØ, \cancel{E}_T is defined as the negative of the vector sum of the calorimeter cell transverse energies (E_T 's).

It is important that the detector is uniform and hermetic, and that the responses to charged hadrons and electrons are similar ($e/\pi \sim 1$). Test beam studies indicated that the linearity of electron and pion response is within 0.5% for energies from 10 GeV to 150 GeV^{2, 3, 4}). The e/π ratio of the detector, shown in Figure 1 for the EC⁵), is close to unity. For *in situ* studies described later, it is also important that the energy resolution of electrons and photons is good, and that their response is well-known. The test beam analyses indicate the resolutions for single particle showers are $0.148/\sqrt{E} \oplus 0.003$ for electrons and $0.470/\sqrt{E} \oplus 0.045$ for charged pions^{2, 3, 4}). The electromagnetic energy scale is determined *in situ* from the ratio of the Z mass as measured at LEP⁶) to that measured at DØ using dielectron final states ($M_Z^{LEP}/M_Z^{DØ}$)^{7, 8}). The linearity for electrons has also been verified *in situ* using π^0 and J/ψ decays⁷).

It is useful to briefly note the nature of jets to help define the calibration goal. The fact that most events display a dijet structure intuitively connects the observed jets to an underlying simple parton interaction. However, it is not easy to associate the jet energy with a specific underlying parton energy (see Figure 2a). The concept of an isolated parton does not exist in the theory of QCD – partons radiate gluons, fragment into hadrons and interact with one another via color flow. This complexity makes jet physics very dependent on the jet definition. The fixed-cone algorithm, which is most commonly used at DØ, clusters energy around a precluster

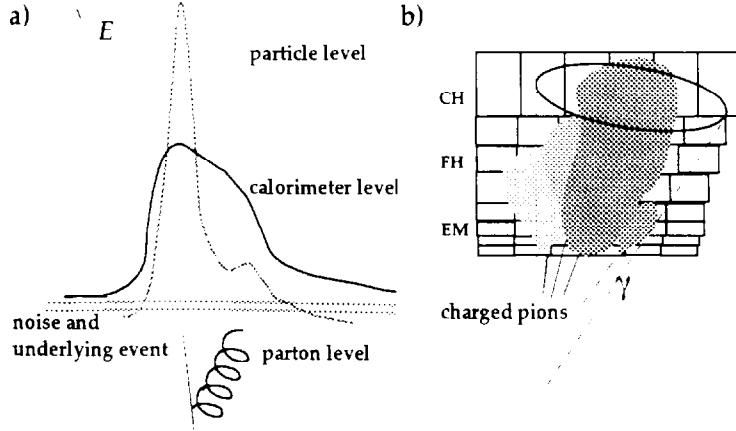


Figure 2: a) Sketch of jets at parton, particle, and calorimeter levels. At the particle level, there is not a clear association of energy to each parton. At the calorimeter level, showering and noise further alter the energy profile. Sketch b) shows a section of calorimeter with individual particle showers. Charged hadrons, in particular, produce wide showers which can spill outside of a jet cone.

axis in a cone of size, $\Delta R = \sqrt{(\Delta\phi)^2 + (\Delta\eta)^2}$, calculates an E_T weighted centroid, and reclusters around that centroid ⁹⁾. ‘Calorimeter jets’ are those jets found with this algorithm after all gluon radiation, fragmentation, and detector effects. We define our jet calibration to compensate only for detector effects so that we attempt to obtain the ‘particle level’ energy of a jet (E_{ptcl}^{jet}) from its measured calorimeter energy (E_{meas}^{jet}). This particle level energy is found with the same algorithm as a matching calorimeter jet but from final state particle energies before detector effects. We could also define a ‘parton level’ jet and attempt to correct back to this but leave that to individual physics analyses.

Our calibration obtains E_{ptcl}^{jet} from E_{meas}^{jet} by correcting for the following:

- I. An energy offset, O , which includes both detector noise and energy from the underlying event.
- II. A change in energy due to showering in the calorimeter, S , which is specific to each jet algorithm.
- III. A change of the energy scale, R (response), due to e/π ^{5, 8)} and energy lost in readout cracks.

Algebraically, we calculate E_{ptcl}^{jet} for a found jet by,

$$E_{ptcl}^{jet} = \frac{(E_{meas}^{jet} - O)}{R(1 - S)}. \quad (1)$$

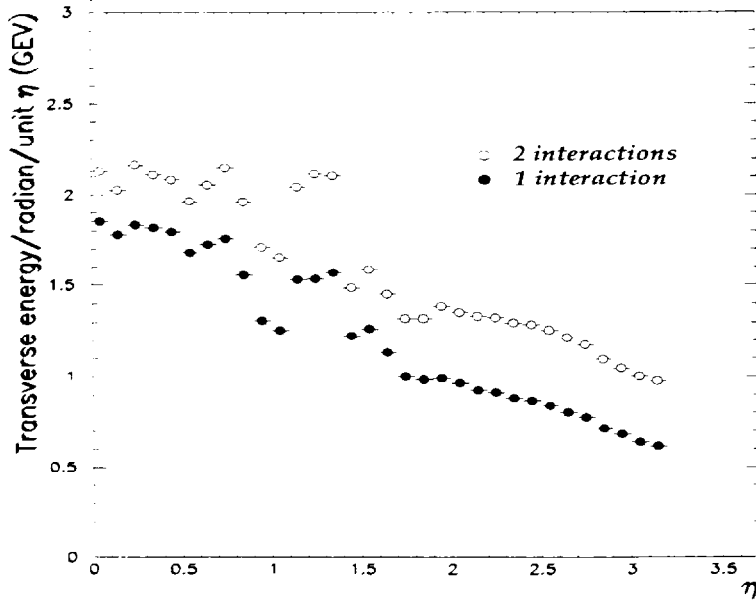


Figure 3: Average E_T density in GeV as a function of calorimeter tower η , for single interaction and double interaction events.

2 Estimation of Offset

Two processes contribute to the energy offset. The absorber plates in the EM and FH portions of the DØ calorimeter are made of depleted uranium whose decay results in a measurable signal. The resulting asymmetric pedestal distribution leaves a net positive energy contribution after a symmetric zero suppression cut, which we label ‘noise’ (N). Additional energy comes from beam remnants and additional $\bar{p}p$ interactions and is termed ‘underlying event’, denoted U .

Figure 3 shows the average E_T density as a function of calorimeter tower η from events satisfying a minimum bias (MB) trigger. The solid circles are from events where only one interaction occurred in each beam crossing. The open circles are from events where two interactions occurred. If the underlying event contribution for two interactions is twice that for single interactions, then the difference between the two histograms in Figure 3 is a measure of the underlying event contribution for a single interaction:

$$U = O_{MB}^{2int.} - O_{MB}^{1int.} \quad (2)$$

The removal of the underlying event contribution from the single interaction energy density gives the noise contribution,

$$N = O_{MB}^{1int.} - U. \quad (3)$$

The systematic error on the underlying event E_T density is $0.2 \text{ GeV/rad/unit} - \eta$, while for noise the uncertainty in the energy density is $0.1 \text{ GeV/rad/unit} - \eta$. These

uncertainties reflect the different values obtained from independent minimum bias samples.

3 Showering

According to our definition of E_{ptcl}^{jet} , no correction is needed when an algorithm is applied at the particle level. Once the fragmentation products strike the calorimeter, however, the observed jet broadens due to the resultant showers and some energy can leak out of, or into, a jet cone (see Figure 2b). To quantify this, central jets are generated with HERWIG¹⁰, and the energies of the fragmentation particles are deposited in the first calorimeter cells intercepted by their momentum vectors. Jet reconstruction is then performed on these cells to produce ‘unshowered’ jets. To produce ‘showered’ jets, the hadrons/photons in the jet are replaced with test beam pions/electrons of the same energy. The particle’s energy is then distributed relative to the intercepted cell as observed in the test beam and jets are reconstructed from these showers. The showered and unshowered jets are matched and the ratio of showered energy to unshowered energy is calculated ($= 1 - S$ in Equation 1). For a cone size of $\Delta R = 0.7$, S varies from 0.01 to 0.0 depending on particle jet energy, while smaller cone sizes have somewhat larger corrections. The preliminary systematic uncertainty is about 1% which is obtained from variations in the estimate of S when calculated in different ways.

4 Jet Response

By ‘jet response’ we refer to the collective response of the calorimeter to all the particles comprising a jet. Our method to determine this has three major components. We use the \cancel{E}_T to determine the relative response between two objects. Direct photon plus jet events then allow us to anchor the jet to an absolute energy scale as a function of the measured jet energy. Finally, the calorimeter’s uniformity is used to extend the energy reach of this analysis.

4.1 Method

Let us consider a dijet event in which one jet is triggered on (‘trigger jet’) and the other is unbiased (‘probe jet’) (see Figure 4a). In order to obtain the response of the probe jet in terms of the \cancel{E}_T , let us consider the three vectors at the particle level: \vec{E}_T^{trig} , \vec{E}_T^{had} , and \vec{E}_T^ν . \vec{E}_T^{had} is the vector sum of all interacting particles in the event outside of the trigger jet ($= \vec{E}_T^{probe} + \vec{E}_T^{jet2}$ of Figure 4b), and \vec{E}_T^ν is the vector sum of all non-interacting particles in the event. In the transverse plane we

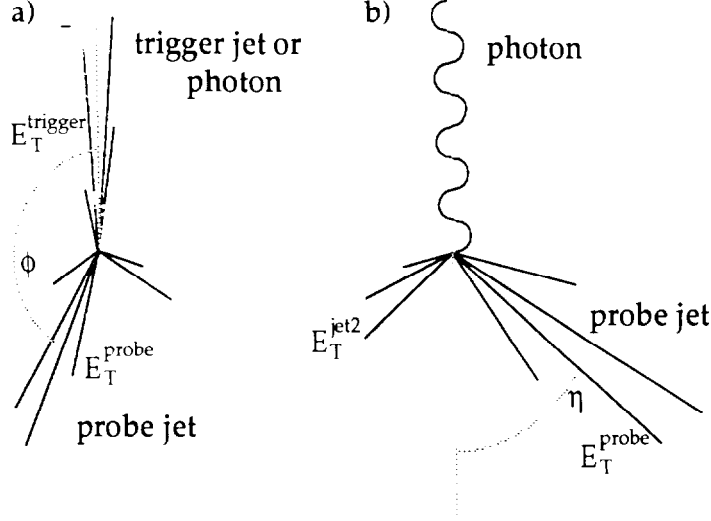


Figure 4: Sketch of the E_T Projection Fraction method showing a) the trigger jet and the recoiling hadronic system. Photon plus jets events, shown in b), are used to provide an absolute calibration of jets.

have

$$\vec{E}_T^{\text{trig}} + \vec{E}_T^{\text{had}} + \vec{E}_T^{\nu} = 0. \quad (4)$$

This becomes

$$R^{\text{trig}} \vec{E}_T^{\text{trig}} + R^{\text{probe}} \vec{E}_T^{\text{had}} = -\vec{E}_T^{\nu} \quad (5)$$

at the calorimeter level, where R^{trig} (R^{probe}) is the response to the trigger (probe) jet. Defining the relative response, $r = R^{\text{probe}} / R^{\text{trig}}$, and assuming \vec{E}_T^{ν} is negligible, we obtain

$$r = 1 + \frac{\vec{E}_T^{\nu} \cdot \hat{n}_T^{\text{trig}}}{E_T^{\text{trig}}} \quad (6)$$

where \hat{n}_T^{trig} is the unit vector in the direction of the trigger jet. When the trigger jet is a calibrated photon, r becomes R^{probe} . We only consider such events in what follows.

If a measured quantity, X , has a poor resolution, the determination of response in terms of X can be biased if one tries to directly plot R^{probe} vs. X . This ‘resolution bias’ arises because, in the case of $X = E_{\text{meas}}^{\text{jet}}$ or E_T^{jet} for instance, the parent distribution is strongly dependent on X at the parton level. However, both the E_T of the photon (E_T^{γ}) and the direction of the probe jet are well-measured so we define the energy estimator, E' , as

$$E' = E_T^{\gamma} \cosh(\eta_{\text{jet}}). \quad (7)$$

E' would be $E_{\text{ptcl}}^{\text{jet}}$ in the absence of additional jets or corrections, and is highly correlated with $E_{\text{meas}}^{\text{jet}}$ in general. Using E' to classify the probe jet, we plot the average $E_{\text{meas}}^{\text{jet}}$ for bins in E' vs. the average R^{probe} in the same bins. For example,

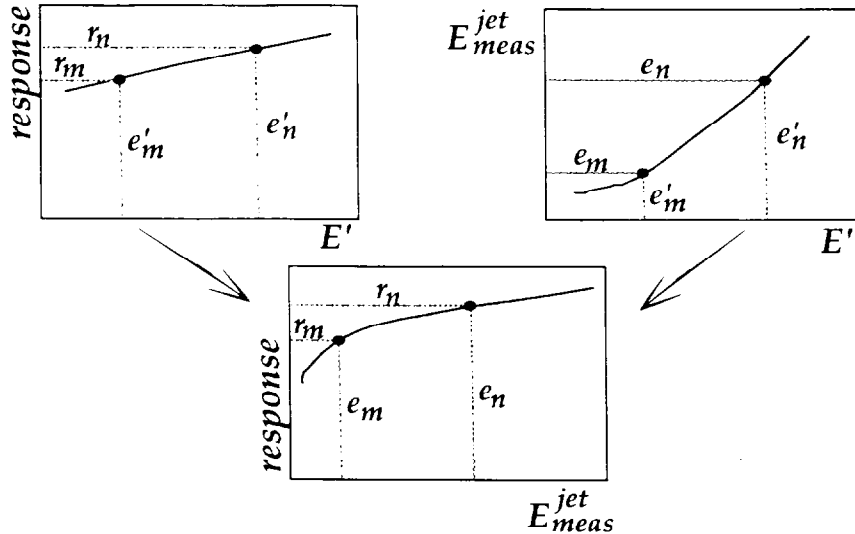


Figure 5: By classifying events by the well-measured variable, E' , we obtain a plot of response *vs.* measured jet energy.

if $R^{probe} = r_n$ when $E' = e'_n$, and $E_{meas}^{jet} = e_n$ when $E' = e'_n$, then $R^{probe} = r_n$ when $E_{meas}^{jet} = e_n$ (see Figure 5). With this procedure we are able to extract response functions with negligible error in a parametric Monte Carlo with jet resolution, photon resolution, falling cross section, and trigger and reconstruction thresholds simulated. Therefore, we assign no systematic error for resolution bias.

4.2 Extending the Jet Energy Reach

For CC jets, we are limited to energy < 150 GeV by the rapidly falling photon cross section. Also, there are large systematic errors involved in the collider data analysis at low E_T (< 20 GeV). To overcome these limitations, we first exploit the uniformity of the detector by using the EC which has higher energy jets. Comparison of the response of jets in CC and EC in the kinematic region in which they overlap indicates consistency of energy scale to within a normalization factor. We use the normalized EC jets to establish the CC response at large energy (up to 350 GeV). To further extend the energy reach, we compare jets in data and an ISAJET¹¹⁾ direct photon sample with full GEANT detector simulation. In the kinematic region where they overlap we find consistency to within a scale factor and renormalize the Monte Carlo points. The total energy range covered is from 10 GeV to 500 GeV.

4.3 Systematic Errors

Initial and final state radiation are sources of uncertainty in the method. When a secondary jet is present and hits the calorimeter, Equation 6 is an approximation

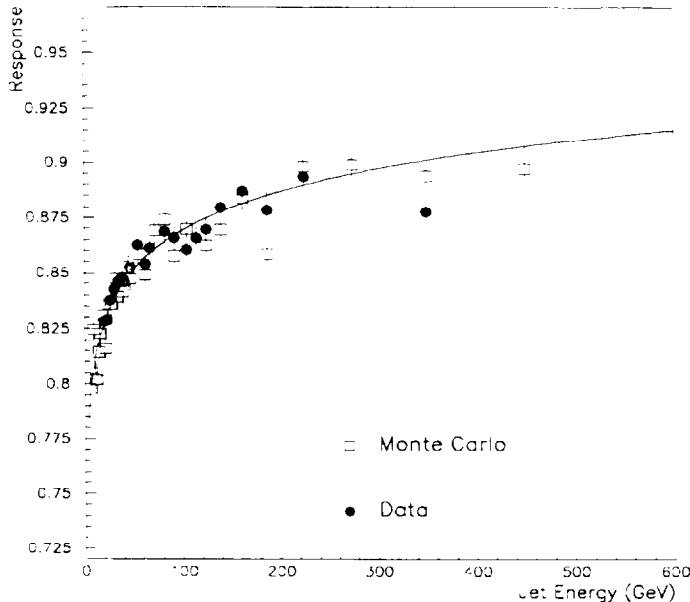


Figure 6: Response, r , of the probe jet relative to the photon *vs.* mean jet energy for Data (solid circles) and Monte Carlo (open squares).

to the probe jet’s response. This ‘topological’ error is determined by measuring the response in a subset of the ISAJET direct photon events generated with only one central jet, and comparing with an inclusive ISAJET sample. Detector simulation was performed for both samples. The estimated bias in measured response is 1% to 2%, depending on jet energy. Significant initial state radiation may be lost down the beampipe. From parametric Monte Carlo studies, the estimated bias in measured response is about 3% when $E_T^\gamma < 20$ GeV, and negligible above 30 GeV.

Backgrounds to direct photons are a source of error for this analysis. We cut on longitudinal and transverse isolation to remove EM jets with significant associated hadronic activity. The residual bias to the measurement is estimated to be $\sim 1.4\%$. We also use the transition radiation detector and dE/dx in tracking chambers to remove W, Z jets background. The remaining W background affects R^{probe} by $\sim 0.5\%$.

Some systematic errors arise from extending the energy reach of the analysis. For the EC data, sensitivity to the number of multiple interactions in an event results in a 2% systematic error. The systematic error on the Monte Carlo/data normalization is about 3.5%.

4.4 Response Curves in Data and Monte Carlo

To choose a function for fitting our response curve, we consider models of hadron showering which give $\epsilon/\pi = [F_{EM} + (1 - F_{EM})R_h]^{-1}$, where R_h is the response of

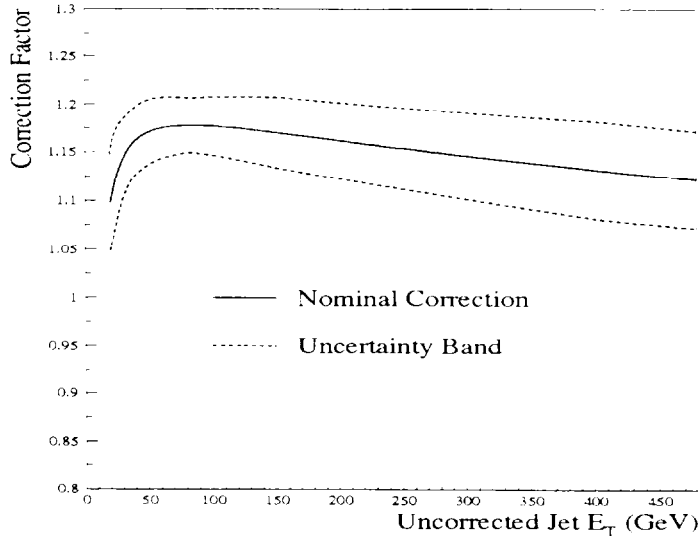


Figure 7: Total jet energy scale correction for central ($|\eta| < 0.5$) jets.

the calorimeter to a particle interacting only via nuclear absorption and F_{EM} is the fraction of real hadron energy deposited via electromagnetically interacting shower products, electrons and photons¹²⁾. The functional form for F_{EM} is $\sim c \cdot \ln(E)$, giving an expected pion response of

$$R_{\pi} = [e/\pi]^{-1} = a + b \cdot \ln(E) \quad (8)$$

relative to that of an electron. Because the test beam data are well-described by this functional form, we use Equation 8 for our jet response fits.

To compare Monte Carlo and data we remove EM scale effects and measure the response of the probe jet *relative to the photon* (ie. r vs. E_{meas}^{jet} , not R^{probe} vs. E_{meas}^{jet}). This is shown in Figure 6 for both samples. The Monte Carlo reproduces both the shape and overall normalization of our *in situ* measurement well within our systematic errors. Also shown is the fit to the Monte Carlo points. An alternate method to predict jet response using test beam particles input into ISAJET and HERWIG particle jets¹³⁾ also agrees within errors.

5 Jet Scale Correction and Verification

The effective overall correction factor is shown in Figure 7 as a function of uncorrected E_T for central jets. The upper and lower dashed lines correspond to 1σ upward and downward excursions of the total error, calculated as the sum in quadrature of all errors. These errors are dominated by systematic errors and there are substantial correlations between errors at different energies.

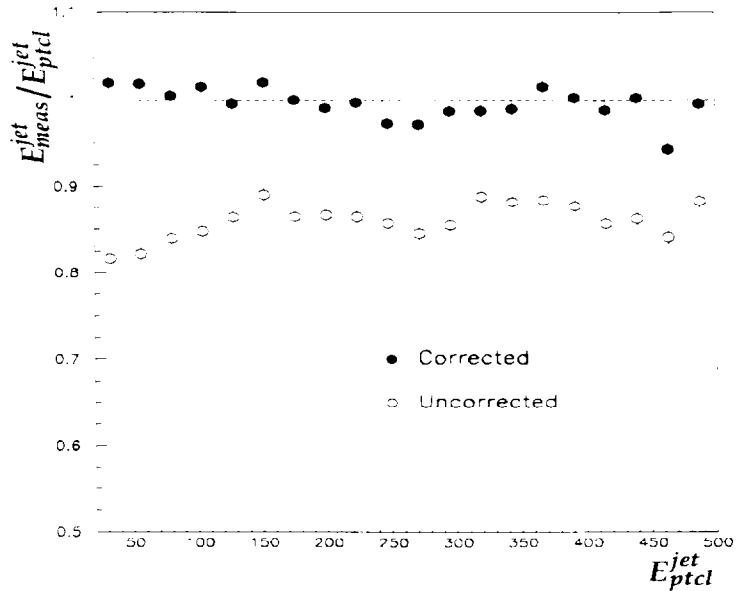


Figure 8: Ratio of reconstructed jet energy to particle jet energy *vs.* particle jet energy before (open circles) and after corrections (solid circles).

We have verified that the total calibration procedure successfully obtains E_{ptcl}^{jet} from E_{meas}^{jet} using jets in the Monte Carlo sample of direct photon events. Figure 8 shows the ratio of calorimeter and particle jet energy *vs.* particle jet energy before corrections (open circles) and after corrections (solid circles). The ratio is consistent with unity after corrections.

6 Conclusions

We have calibrated jets in the $D\bar{O}$ calorimeters to compensate for noise, spectator interactions, response, and showering. The overall correction is between 10% and 18% for 0.7 cone jets above 20 GeV. The total error is about 5% below 20 GeV and above 300 GeV, and about 2.5% at 80 GeV. The calibration is constrained by data from 20 GeV to 350 GeV, with the portion above 150 GeV coming from EC jets. Above 350 GeV and below 20 GeV Monte Carlo data are used. Predictions of jet response in the Monte Carlo agrees with that measured in the data within errors. An explicit comparison in Monte Carlo samples of calorimeter and matching particle jet energies indicates we have correctly calculated E_{ptcl}^{jet} within errors.

We thank the staffs at Fermilab and the collaborating institutions for their contributions to the success of this work, and acknowledge support from the Department of Energy and National Science Foundation (U.S.A.), Commissariat à L’Energie Atomique (France), Ministries for Atomic Energy and Science and Technology Policy (Russia), CNPq (Brazil), Departments of Atomic Energy and Science

and Education (India), Colciencias (Colombia), CONACyT (Mexico), Ministry of Education and KOSEF (Korea), CONICET and UBACyT (Argentina), and the A.P. Sloan Foundation.

References

1. S. Abachi *et al.*, (DØ Collab.), Nucl. Instr. and Meth., **A338** (1994) 185.
2. S. Aronson *et al.*, Nucl. Instr. and Meth., **A269** (1988) 492.
3. M. Abolins *et al.*, Nucl. Instr. and Meth., **A280** (1989) 36.
4. S. Abachi *et al.*, Nucl. Instr. and Meth., **A324** (1992) 53.
5. H. Aihara *et al.*, (DØ Collab.), Nucl. Instr. and Meth., **A325** (1993) 393.
6. P. Renton, "Precision Tests of Electroweak Theories", Lepton-Photon Conference, Beijing, China (1995), OUNP-95-20.
7. S. Abachi *et al.*, (DØ Collab.), Fermilab Report No. FERMILAB-PUB-96/177-E, 1996, submitted to Phys. Rev. Lett.
J. Kotcher, these proceedings.
8. J. Kotcher, Proc. of the 1994 Beijing Calor. Symp., IHEP - Chinese Acad. of Sci., Beijing, China, Oct. 25-27, 1994, pp. 144-158.
9. S. Abachi *et al.*, (DØ Collab.), Phys. Lett. **B357** (1995) 500-508.
10. G. Marchesini and B.R. Webber, Nucl. Phys. **B310** (1988) 461, vers. 4.6.
11. F. Paige and S. Protopopescu, Report No. BNL38034, 1986 (unpub.), vers. 7.06.
12. D. Green, Fermilab Report No. FERMILAB-TM-1958, 1996.
C. Fabjan, Calorimetry in High Energy Physics, in Experimental Techniques in High Energy Physics, Ed. T. Ferbel, Addison-Wesley, 1987.
13. D. Stewart, Proc. of the 3rd Int. Conf. on Calor. in High Energy Phys., Corpus Christi, Texas, Sep. 29 - Oct. 2, 1992, pp. 741.